AJNR Am J Neuroradiol 19:1373–1377, August 1998

MR Imaging and Localized Proton MR Spectroscopy in Late Infantile Neuronal Ceroid Lipofuscinosis

Dietmar Seitz, Wolfgang Grodd, Alexandra Schwab, Uwe Seeger, Uwe Klose, and Thomas Nägele

PURPOSE: **Late juvenile neuronal ceroid lipofuscinosis (NCL) is a lysosomal neurodegenerative disorder caused by the accumulation of lipopigment in neurons. Our purpose was to characterize the MR imaging and spectroscopic findings in three children with late infantile NCL.**

METHODS: **Three children with late infantile NCL and three age-matched control subjects were examined by MR imaging and by localized MR spectroscopy using echo times of 135 and 5. Normalized peak integral values were calculated for *N*-acetylaspartate (NAA), choline, creatine, *myo*-inositol, and glutamate/glutamine.**

RESULTS: **MR imaging revealed volume loss of the CNS, most prominently in the cerebellum. The T2-weighted images showed a hypointense thalamus and hyperintense periventricular white matter. Proton MR spectra revealed progressive changes, with a reduction of NAA and an increase of *myo*-inositol and glutamate/glutamine. In long-standing late infantile NCL, *myo*-inositol became the most prominent resonance. Lactate was not detectable.**

CONCLUSION: **MR imaging in combination with proton MR spectroscopy can facilitate the diagnosis of late infantile NCL and help to differentiate NCL from other neurometabolic disorders, such as mitochondrial or peroxisomal encephalopathies.**

Neuronal ceroid lipofuscinosis (NCL) refers to a heterogeneous group of inherited neurodegenerative disorders characterized by the accumulation of lipopigment within the lysosomes of neurons and other tissues (1). Six main types have been identified: infantile, late infantile (Jansky-Bielschowsky disease), juvenile, adult recessive, adult dominant, and early juvenile. In addition, several subtypes of NCL have been classified (2). The biochemical defect in late infantile NCL is an abnormal catabolism of subunit c, a part of the mitochondrial adenosine triphosphate (ATP) synthase complex (3).

Localized proton MR spectroscopy of the brain can be used as an additional diagnostic tool in conjunction with MR imaging and is especially indicated in children with suspected neurodegenerative or metabolic disorders (4, 5). For example, if proton MR spectra of the basal ganglia reveal lactate despite normal MR imaging findings (6), then a diagnosis of a mitochondrial disorder will be more likely and will encourage the performance of a muscle biopsy for final assessment.

We report the MR imaging and spectroscopic changes in three children with late infantile NCL.

Methods

Three children (two boys and one girl) were examined at the age of 4, 4, and 7 years, respectively. Two patients were siblings (cases 2 and 3). Patients 1 and 2 (each 4 years old) had a 1.5-year history of seizurelike episodes and muscular hypotonia; however, patient 1 was additionally handicapped by a severe ataxia. Patient 3 (7 years old) had a 4.5-year history of a mental handicap, inability to walk, and several myoclonic seizures per day. In all three cases the diagnosis of late infantile NCL was confirmed by results of a skin biopsy (fibroblasts).

The MR imaging and proton MR spectroscopic examinations were requested for evaluation of intracerebral changes. To enable a detailed comparison, MR spectra of three age-matched children (two boys and one girl; 5 to 8 years old) were selected from a larger control population who had neither intracerebral disease nor neurologic abnormalities.

The examinations were performed on a 1.5-T whole-body system using a standard circularly polarized head coil and actively shielded gradients. MR imaging consisted of axial and sagittal T1-weighted spin-echo (SE) sequences with parameters of 450/12/1 (TR/TE/excitations) and a 230-mm field of view

Received July 15, 1997; accepted after revision January 22, 1998.

From the Departments of Neuroradiology (D.S., W.G., U.S., U.K., T.N.) and Neuropediatrics (A.S.), University of Tübingen, Germany.

Address reprint requests to Dietmar F. Seitz, MD, Section of Experimental MR of CNS, Department of Neuroradiology, University of Tübingen, Hoppe-Seyler-Str. 3, D 72076 Tübingen, Germany.

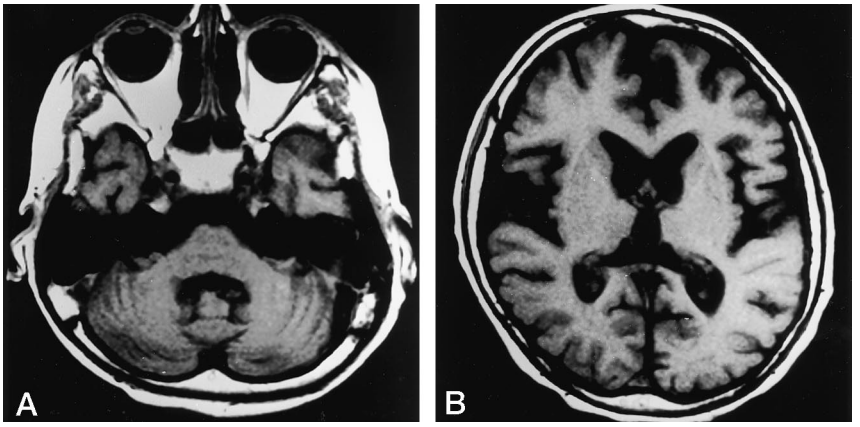

FIG 1. *A* and *B*, Axial T1-weighted images (450/12/1) in patient 3. In late infantile NCL, a marked cortical atrophy is seen, most prominently in the cerebellum (*A*) and frontal lobes (*B*). Although this patient had the longest history of late infantile NCL, no signal intensity changes are seen in the white and gray matter.

(FOV). The section thickness was 5 mm with a 1-mm gap. An axial T2-weighted (double SE) sequence was added with parameters of 3000/45,90/2 and a 230-mm FOV.

For proton MR spectroscopy, the volume of interest was placed in the right central parietal lobe, containing predominantly white matter (volume, 9.3 cm^3). An SE sequence (1500/135/128) and a self-designed stimulated-echo acquisition mode (STEAM) sequence (7) (1500/5/128) with a mixing time of 5 milliseconds was used for localized spectroscopy. Localized shimming and water suppression were done individually for both sequences.

Spectral postprocessing included 4k zero-filling, gaussian apodization, Fourier transformation, eddy current correction, water reference processing, frequency shift correction, and phase and baseline correction. Peak integral values were determined by a curve fit algorithm for creatine/phosphocreatine (Cr) (3.03 ppm), choline-containing compounds (Cho) (3.2 ppm), lactate (1.3 ppm), *N*-acetylaspartate (NAA) (2.0 ppm), *myo*-inositol (mI) (3.56 ppm), and glutamate/glutamine (Glx) (3.6 to 3.8 ppm). To normalize for individual differences, the residual water signal was subtracted and all integral values were normalized to the internal Cr peak before evaluation.

Results

Consistent with the duration of late infantile NCL, MR imaging showed various degrees of cortical atrophy in all three patients. The most affected regions were the frontal lobes and cerebellum. Gray and white matter had normal signal intensity on T1-weighted images (Fig 1). The T2-weighted images of patients 1 and 2 revealed only a minor increase in signal intensity in the periventricular white matter (Fig 2A–C). Patient 3, with the longest history of late infantile NCL, had the most significant volume loss and the most prominent T2-weighted white matter hyperintensity, affecting all myelinated regions (Fig 2D–F). Progressive T2-weighted hyperintensity affected the optic radiation and internal capsule. The degree of hypointensity within the thalamus was variable among patients.

The spectra in patients with late infantile NCL differed from those of the control subjects (Fig 3), with the greatest variation from normal related to duration of the disease. The spectra at long TEs (135 milliseconds) showed a mean NAA/Cr decrease to a ratio of 1.15 in patients with NCL as compared with 1.99 in the control group (Table 1). This was equivalent to a reduction of 42%. Patient 3 had the lowest NAA/Cr ratio, at 0.89 (−55%). The spectra at short TEs (5 milliseconds) showed a mean reduction in NAA/Cr to 1.09 (−28%) in patients (Table 2). Patient 3 had the lowest level of NAA/Cr, at 0.72 (−53%), whereas patients 1 and 2 had a reduction to only 1.39 (−9%) and 1.17 (−23%), respectively. At long- and short-TE spectroscopy, the degree of NAA reduction corresponded well with clinical symptoms and duration of late infantile NCL. At both TEs, the Cho/Cr ratios showed only minor differences between patients and control subjects. Lactate was not detectable in either the early or progressive stages of late infantile NCL. The most obvious change was seen for mI in short-TE (5-millisecond) spectra. The mean mI/Cr ratio was elevated to 1.25 (+74%) in the patients (Table 2). The changes in mI/Cr ratios were also in concordance with the severity of disease. Patient 3 had the highest level of mI/Cr, at 1.5 (+108%) (Fig 3D). The Glx/Cr ratios were also increased in the patients, to 1.53 (+65%), but there was no clear correlation between that increase and the patients' symptoms or duration of disease.

Discussion

Children with late infantile NCL are healthy until the age of 3 years, when a mixed seizure disorder develops and electroencephalographic changes occur (1, 8). Ataxia, visual problems, and hypotonia are other early manifestations (1, 9).

CT and MR imaging in patients with NCL show global brain atrophy of gray and white matter (8, 10–15) but no distinct disorder of myelination. As the disease progresses, cerebellar atrophy becomes dominant and diffuse periventricular white matter hyperintensities are found on T2-weighted MR images.

Clinical features and changes on MR images can help in the diagnosis of NCL and in differentiating the various types of NCL. The late infantile type of NCL may be differentiated from the infantile and juvenile NCL types on the basis of symptom onset. Clinical onset occurs at 2 to 3 years of age in infantile NCL, at 2.5 to 4 years in late infantile NCL, and at 4 to 7 years in juvenile NCL; however, subtypes can lead to an overlap in presentation (1, 2, 8, 9). Only in the infantile form of NCL do the changes on MR

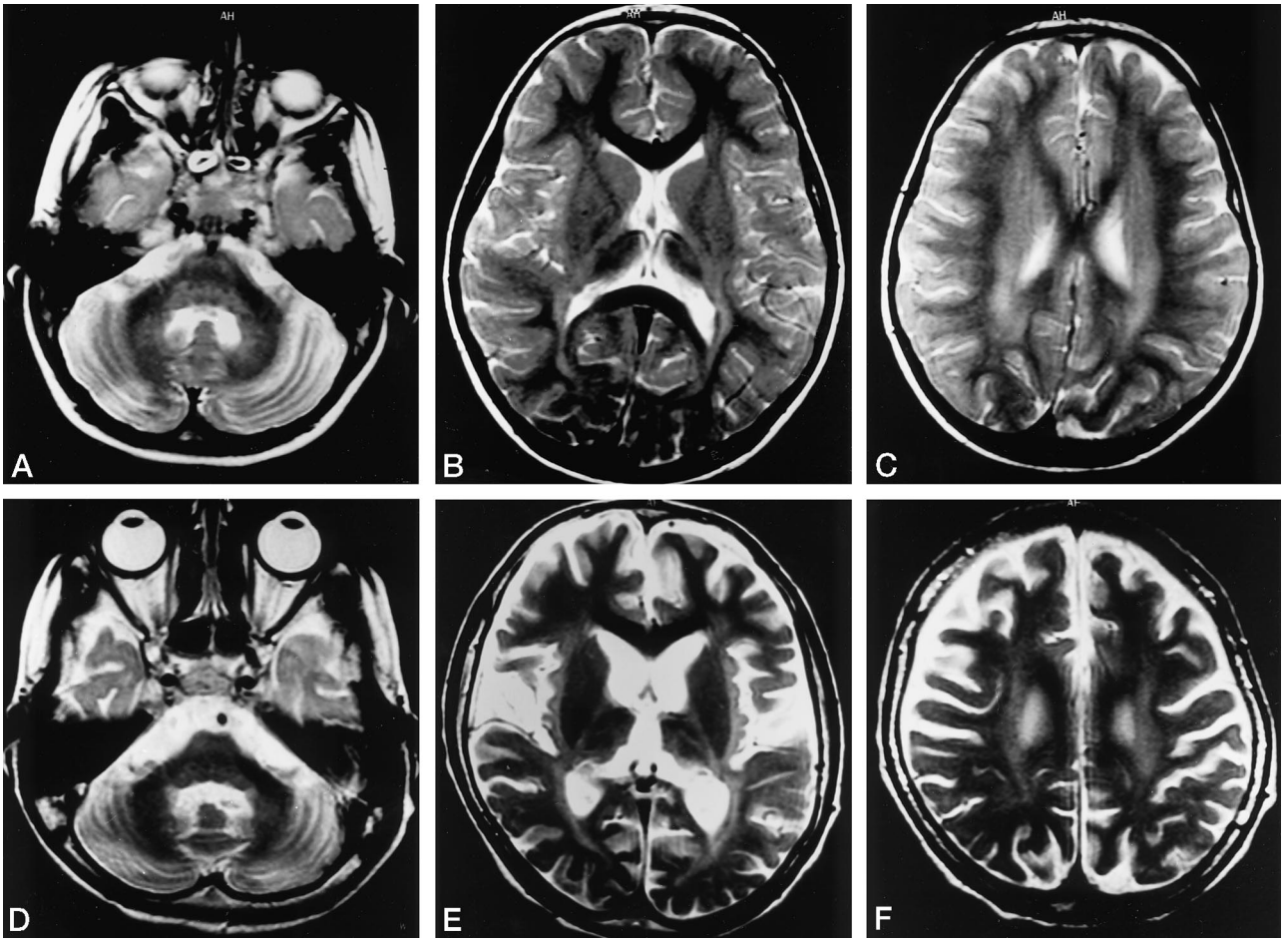

FIG 2. Axial T2-weighted images (3000/90/2) in the early (patient 2, *A–C*) and progressed (patient 3, *D–F*) stages of late infantile NCL. The progressing cerebellar atrophy results in enlargement of the cerebellopontine cistern and the fourth ventricle (*A* and *D*). There is a hyperintense periventricular band, an increased signal in the internal capsule, and a hypointense thalamus on images through the basal ganglia (*B* and *E*). The gray matter becomes atrophic in combination with a hyperintense white matter as the disease progresses (*C* and *F*).

images precede clinical symptoms; in late infantile and juvenile NCL, clinical symptoms precede the MR findings by up to a year.

In NCL, continuing neuronal death leads to progressive axonal (wallerian) degeneration and gliosis (10, 11). These alterations may explain the decreased signal of gray matter as well as the hyperintense signal of white matter on T2-weighted images (8, 12, 13). The various NCL types often have characteristic MR features. Generalized CNS atrophy with cerebellar involvement and white matter hyperintensities on T2-weighted images are typical in late infantile NCL. In the classical form of late infantile NCL, the thalamus and basal ganglia appear normal on T2-weighted images, whereas in children with subforms of late infantile NCL, the thalamus is hypointense (14). The hypointense T2-weighted signal in the thalamus in all our patients was in concordance with the ultrastructural diagnosis of a variant subtype of late infantile NCL. At the beginning of infantile NCL, the typical MR findings are that of a generalized cerebral atrophy and hypointense thalamus as well as a thin periventricular high-signal band on T2-weighted images (15). As the infantile NCL type progresses, the cerebral atrophy becomes extreme and the signal intensity of the entire white matter region becomes higher than that of gray matter. MR changes in juvenile NCL include evidence of a mild generalized atrophy and increased signal intensity of the entire white matter region on T2-weighted images (16).

The difficulty in establishing the diagnosis of NCL is due to the fact that this is a group of diseases, including various subforms of the known classical types, rather than a single entity (2). Hence, there is a great deal of variability in onset and types of symptoms, as well as in MR features. Both the clinical and MR findings can be equivocal in some patients; therefore, diagnosis has to be established by electron microscopic examination of lymphocytes or fibroblasts, gained by a skin punch biopsy.

Proton MR spectroscopy can provide biochemical information by the noninvasive in vivo measurement of cerebral metabolites. An NAA/Cr reduction in CNS reflects neuronal disintegration, and was obvious in our patients. The degree of neuronal damage suggested by spectroscopy was in accord with the duration of late infantile NCL by history. Neuronal damage in late infantile NCL may be due to repetitive seizures or to an excess of lysosomal storage material. Patients with a long-standing history of epilepsy show

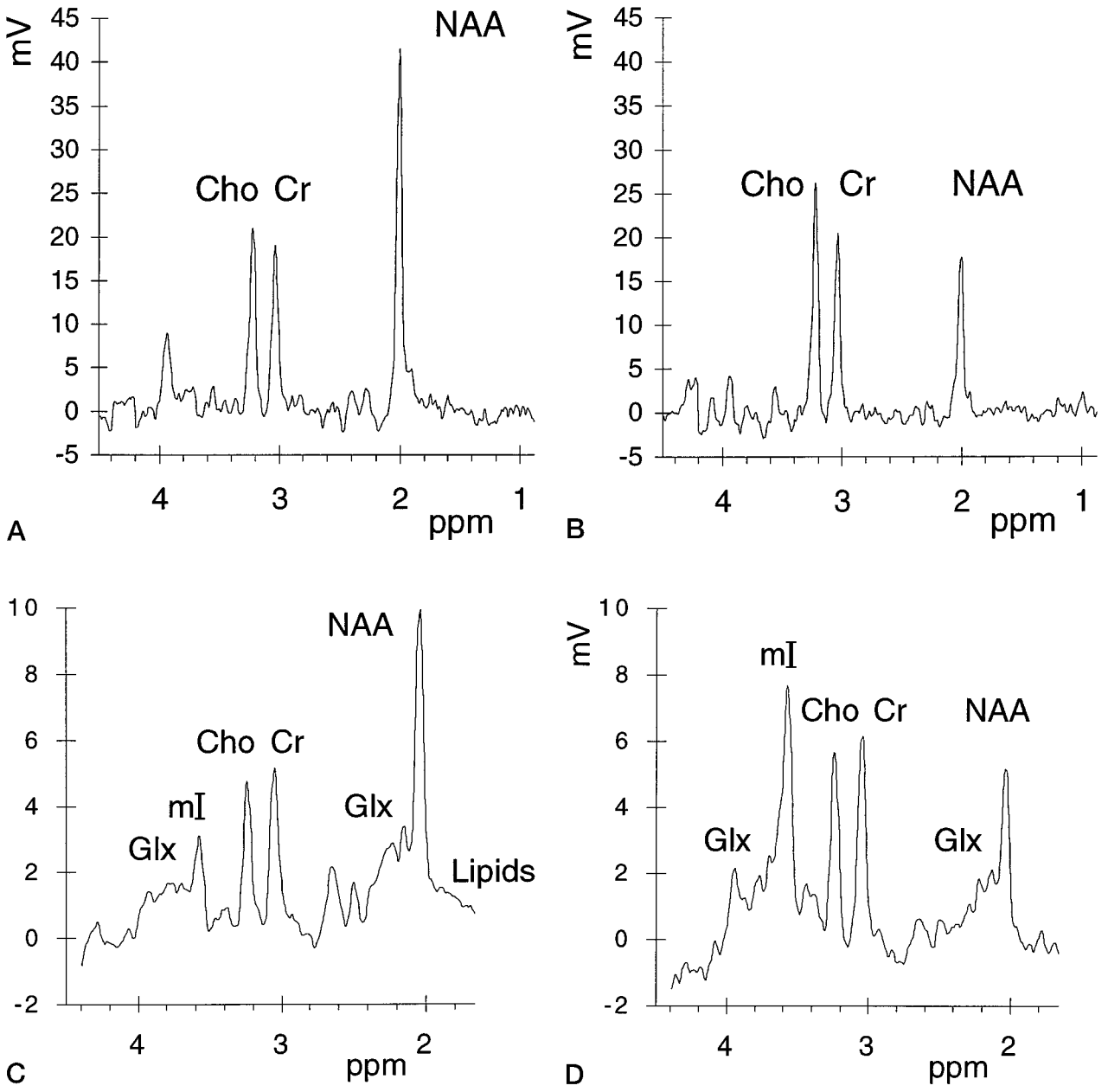

FIG 3. Volume-selective proton MR spectra (1500/135,5/128) of occipital white matter in a control subject and in the progressed stage of late infantile NCL (patient 3).

A, The long-TE (135 milliseconds) spectrum in the control subject shows the resonances of NAA, Cho, and Cr.

B, In the progressed stage of late infantile NCL, the long-TE spectrum shows a decrease of NAA, no changes in Cho, and no detectable lactate.

C, The short-TE (5 milliseconds) spectrum in the control subject additionally shows the resonances of lipids, mI, and Glx.

D, The short-TE spectrum in late infantile NCL reveals mI as the most prominent signal.

a decreased NAA signal and an increased Cho signal. In the posticteral state, proton MR spectroscopy additionally detects lactate (17). The nearly unchanged Cho/Cr ratio and the absence of lactate make the neuronal loss due to repetitive seizures unlikely. For these reasons, our results seem to support the hypothesis that the neuronal and axonal loss is due to an impaired cell function, resulting in neuronal death and gliosis. An increased number of glial cells results in increased mI levels. Through regulation of intra/extracellular mI levels, glial cells control cerebral osmotic regulation (18). In patients, the calculated Glx/Cr ratios were uniformly increased, but there was no concordance with the patients' clinical condition. The α-resonances of Glx are both at 3.6 to 3.8 ppm and overlay each other. Differentiation of the two metabolites is not possible with normal proton MR spectroscopy. Additionally, other metabolites, such as macromolecules and glucose, have their resonance in this region and can be confused with an increase in Glx.

We found two reports on the use of proton MR

TABLE 1: Integral values of proton MR spectroscopy at TE = 135

	Control Subjects	Patients	Patient 1	Patient 2	Patient 3
NAA/Cr	1.99 ± 0.22	1.15 ± 0.26	1.15	1.41	0.89
Cho/Cr	1.07 ± 0.04	1.13 ± 0.18	0.92	1.19	1.27

Note.—NAA, *N*-acetylaspartate; Cho, choline-containing compounds; Cr, phosphocreatine/creatine. All integral values were normalized to the internal Cr peak.

TABLE 2: Integral values of proton MR spectroscopy at TE = 5

	Control Subjects	Patients	Patient 1	Patient 2	Patient 3
NAA/Cr	1.52 ± 0.04	1.09 ± 0.34	1.17	1.39	0.72
Cho/Cr	0.81 ± 0.04	0.91 ± 0.13	0.77	1.02	0.94
mI/Cr	0.72 ± 0.02	1.25 ± 0.23	1.04	1.20	1.50
Glx/Cr	0.93 ± 0.12	1.53 ± 0.05	1.47	1.57	1.55

Note.—NAA, *N*-acetylaspartate; Cho, choline-containing compounds; Cr, phosphocreatine/creatine; mI, *myo*-inositol; Glx, glutamate/glutamine. All integral values were normalized to the internal Cr peak.

spectroscopy in NCL. Confort-Gouny et al (19) reported a major reduction in NAA, no lactate, and an increased mI signal in the thalamus of a 4-year-old child with infantile NCL. Brockmann et al (20) found a reduction in NAA and an increase in mI in combination with a positive lactate level in the classical type of late infantile NCL. However, their reported lactate peak consisted mainly of lipid resonances. A reduced NAA signal, a prominent mI peak, and no detectable lactate seem to be more consistent with (late) infantile NCL.

Typical changes of metabolites can facilitate the diagnosis of hereditary and acquired brain disorders in children (4, 5). Changes in cerebral metabolites can also help to monitor metabolic changes during therapeutic procedures (6). Neurometabolic disorders can produce typical changes in the composition of cerebral metabolites (4–6). For example, children with mitochondrial dysfunction of the Leigh type show T2-weighted hyperintensities in the basal ganglia, a decreased NAA/Cho ratio, and positive lactate (5, 6). An increased mI and NAA signal, despite neuronal damage, can only be found in Canavan disease, caused by an aspartocyclase defect (21). Peroxisomal disorders, like adrenoleukodystrophy, reveal white matter hyperintensities on T2-weighted MR images and a virtual absence of NAA in severely affected areas, increased mI, and positive lactate on MR spectra. Therefore, MR spectroscopy can give additional hints to the diagnosis in children with neurometabolic disorders.

Summary

The diagnosis of late infantile NCL disease has to be considered in children with cerebellar atrophy (hypointense signal involving the thalamus), periventricular T2-weighted hyperintensities in combination with reduced NAA, and distinctly increased mI on proton MR spectra.

References

1. Nardocci N, Verga ML, Binelli S, Zorzi G, Angelini L, Bugiani O. **Neuronal ceroid-lipofuscinosis: a clinical and morphological study of 19 patients.** *Am J Med Genet* 1995;57:123–141
2. Dyken P, Wisniewski K. **Classification of the neuronal ceroid-lipofuscinoses: expansion of the atypical form.** *Am J Med Genet* 1995;57:150–154
3. Kominami E, Ezaki J, Wolfe LS. **New insight into lysosomal protein storage disease: delayed catabolism of ATP synthase subunit c in Batten disease.** *Neurochem Res* 1995;20:1305–1309
4. Aria Tzika A, Ball WS, Vigneron DB, Dunn RS, Kirks DR. **Clinical proton MR spectroscopy of neurodegenerative disease in childhood.** *AJNR Am J Neuroradiol* 1993;14:1267–1281
5. Grodd W, Krägeloh-Mann I, Klose U, Sauter R. **Metabolic and destructive brain disorders in children: findings with localized proton MR spectroscopy.** *Radiology 1991;181:173–181*
6. Krägeloh-Mann I, Grodd W, Schöning M, Marquard K, Nägele T, Ruitenbeek W. **Proton spectroscopy in five patients with Leigh's disease and mitochondrial enzyme deficiency.** *Dev Med Child Neurol* 1993;35:769–776
7. Seeger U, Klose U, Seitz D, Naegele T, Lutz 0, Grodd W. **Proton spectroscopy of human brain with very short echo time using high gradients.** *Magn Reson Imaging* 1998;16:55–62
8. Knaap MS, Valk J. *Magnetic Resonance of Myelin, Myelination, and Myelin Disorders.* 2nd ed. Berlin: Springer; 1995;44:252–258
9. Boustany R-M. **Neurology of the neuronal ceroid-lipofuscinoses: late infantile and juvenile types.** *Am J Med Genet* 1992;42:533–535
10. Barkovich AJ. *Pediatric Neuroimaging.* 2nd ed. New York: Raven Press; 1995:55–106
11. Kuhn MJ, Johnson KA, Kenneth RD. **Wallerian degeneration: evaluation with MR imaging.** *Radiology* 1988;168:199–202
12. Kendall BE. **Disorders of lysosomes, peroxisomes, and mitochondria.** *AJNR Am J Neuroradiol* 1992;13:621–653
13. Osborne AG. **Inherited metabolic, white matter, and degenerative diseases of the brain. In: Osborne AG, ed.** *Diagnostic Neuroradiology.* St Louis: Mosby; 1994:716–746
14. Peterson B, Handwerker M, Huppertz H-I. **Neuroradiological findings in classical late infantile neuronal ceroid-lipofuscinosis.** *Pediatr Neurol* 1996;15:344–347
15. Vanhanen S-L, Raininko R, Autti T, Santavuori P. **MRI evaluation of the brain in infantile neuronal ceroid-lipofuscinosis, 2: MRI findings in 21 patients.** *J Child Neurol* 1995;10:444–450
16. Autti T, Raininko R, Vanhanen SL, Santavuori P. **MRI of neuronal ceroid lipofuscinosis, I: cranial MRI of 30 patients with juvenile neuronal ceroid lipofuscinosis.** *Neuroradiology* 1996;38:476–482
17. Novotny EJ. **Overview: the role of NMR spectroscopy in epilepsy.** *Magn Reson Imaging* 1995;13:1171–1173
18. Brand A, Richter-Landsberg C, Leibfritz D. **Multinuclear NMR studies on the energy metabolism of glial and neuronal cells.** *Dev Neurosci* 1993;15:289–298
19. Confort-Gouny S, Chabrol B, Vion-Dury J, Mancini J, Cozzone PJ. **MRI and localized proton MRS in early infantile form of neuronal ceroid lipofuscinosis.** *Pediatr Neurol* 1993;9:57–60
20. Brockmann K, Pouwels PJW, Christen H-J, Frahm J, Hanefeld F. **Localized proton magnetic resonance spectroscopy of cerebral metabolic disturbances in children with neuronal ceroid lipofuscinosis.** *Neuropediatrics* 1996;27:242–248
21. Grodd W, Krägeloh-Mann I, Petersen D, Trefz FK, Harzer K. **In vivo assessment of N-acetylaspartate in brain in spongy degeneration (Canavan's disease) by proton spectroscopy.** *Lancet* 1990; 336:437–438